Kinetics and Mechanism of O (^{3}P) Reaction with CH_3CHF_2: A Theoretical Study

Qingzhu Zhang,[†,‡] R. Q. Zhang,*[,†] and Yueshu Gu[‡]

Centre of Super-Diamond Films (COSDAF) & Department of Physics and Materials Sciences, City University of Hong Kong, Hong Kong SAR, China and School of Chemistry and Chemical Engineering, Shandong University, China

Received: August 17, 2003; In Final Form: November 22, 2003

The reaction of atomic O (^{3}P) with CH_3CHF_2 has been studied theoretically using ab initio direct dynamics methods for the first time. This reaction takes place through two possible channels: H abstraction from the methyl group (CH_3) and H abstraction from the methyne group (CH). Two nearly degenerate saddle points of ^{3}A″ and ^{3}A′ symmetries have been located for each hydrogen abstraction channel. At the QCISD(T)/6-311+G(3df,2p)//MP2/6-311G(d,p) level, the potential barrier of H abstraction from the CH_3 group is about 5 kcal/mol higher than that of H abstraction from the CH group. Changes of geometries, generalized normal-mode vibrational frequencies, and potential energies along the reaction paths for all the channels are discussed and compared. On the basis of the ab initio data, the rate constants of each channel have been deduced by canonical variational transition-state theory (CVT) with small-curvature tunneling (SCT) correction method over a wide temperature range of 200∼3000 K. The theoretical results have been compared with available experimental data. The kinetics calculations show that the variational effect is small, and in the low-temperature range the small curvature tunneling contribution is important for all the channels. The detailed branching ratios have been discussed.

1. Introduction

The importance of haloalkanes in atmospheric chemistry is well-established.[1−3] As is well-known, the burning of haloalkanes has the potential to generate products such as phosgene, which are more hazardous than haloalkanes themselves. To develop a more efficient and less hazardous incineration of industrial wastes, it is necessary to understand all aspects of this combustion process, in particular the incineration mechanism. Fundamental knowledge of mechanisms, specific pathways, and rate constants of important elementary reactions, including those haloalkanes, is of key importance to the success of kinetic modeling of these systems.

Reactions of atomic O (^{3}P) with haloalkanes are important initial steps of haloalkanes combustion.[4] Experimentally, the kinetics of such reactions of O (^{3}P) with haloalkanes has been extensively studied[5−13] and it continues to receive considerable attention. The extensive experimental work contrasts with the lack of theoretical studies. In fact, the development of computational power allows now the high-level theoretical study of chemical reactions being conducted with fairly large systems, predicting, for example, the reaction pathways in thin-film deposition[14] and biological system[15] and important chemical properties of nanosized materials.[16] In this paper, we present a theoretical study on the reaction of O (^{3}P) with CH_3CHF_2 over a wide temperature range of 200∼3000 K. We have first revealed theoretically the reaction mechanism. It was followed by kinetics calculations for the reaction of O (^{3}P) with CH_3CHF_2. Several important features of this study are as follows. (1) The experimentally suggested reaction mechanism has been confirmed at high levels of ab initio molecule orbital theory. (2) The energy profile surfaces have been generated at the QCISD(T)/6-311+G(3df,2p)//MP2/6-311G(d,p) theory level. (3) The rate constants have been studied in the temperature range from 200 to 3000 K using interpolated canonical variational transition-state theory (CVT)[17−19] and the centrifugal-dominant, small-curvature tunneling approximation (SCT),[20] using information on the reactants, products, saddle point, and extra points along the minimum energy path obtained from ab initio calculations. (4) The non-Arrhenius expressions have been fitted. (5) The calculated rate constants are compared with the available experimental values.

2. Computation Methods

High-level ab initio calculations have been carried out using Gaussian 98 package[21] for the reaction of O (^{3}P) with CH_3CHF_2. In the entire paper, MP2 and QCISD(T) denote the unrestricted versions, UMP2 and UQCISD(T). The geometrical parameters of the reactant, saddle points, and products have been optimized at the MP2/6-311G(d,p) level. The vibrational frequencies have been calculated at the same level to determine the nature of the stationary points, the zero-point energy (ZPE), and the thermal contributions to the free energy of activation. Each saddle point was verified to connect the designated reactants and products by performing an intrinsic reaction coordinate (IRC) analysis. At the MP2/6-311G(d,p) level, the minimum energy paths (MEP) were constructed, starting from the respective saddle point geometries and going downhill to both the asymptotic reactant and product channel with a gradient step size of 0.02 amu$^{1/2}$ Bohr, for all the channels. The force constant matrixes of the stationary points and selected nonstationary points near the saddle point along the MEP were also calculated to do further kinetics calculations.

Although satisfactory geometrical parameters and the frequencies of various species can be determined at the MP2/-

* Corresponding author. E-mail: aprqz@cityu.edu.hk.
† City University of Hong Kong.
‡ Shandong University.

10.1021/jp036446u CCC: $27.50
Published on Web 01/17/2004

6-311G(d,p) level of theory, subsequent kinetics calculations would require highly accurate energies. Hence, an even higher level of theory, QCISD(T), and a more flexible basis set, 6-311+G(3df,2p), were employed for this purpose.

Ab initio calculations provide essential information to calculate the variational rate constant with the inclusion of tunneling effect contribution. The canonical variational theory (CVT) rate constant[17−19] for temperature T is given by

$$k^{\mathrm{CVT}}(T, s) = \min k^{\mathrm{GT}}(T, s) \tag{1}$$

in which

$$k^{\mathrm{GT}}(T,s) = \frac{\sigma k_{\mathrm{B}} T}{h} \frac{Q^{\mathrm{GT}}(T,s)}{\Phi^{\mathrm{R}}(T)} e^{-V_{\mathrm{MEP}}(s)/k_{\mathrm{B}}T} \tag{2}$$

where, $k^{\mathrm{GT}}(T, s)$ is the rate constant in generalized transition-state theory at the dividing surface s, with σ being the symmetry factor accounting for the possibility of more than one symmetry-related reaction path, k_{B} the Boltzmann's constant, h the Planck's constant, $\Phi^{\mathrm{R}}(T)$ the reactant partition function per unit volume (excluding symmetry numbers for rotation), and $Q^{\mathrm{GT}}(T, s)$ the partition function of a generalized transition state at s with a local zero of energy at $V_{\mathrm{MEP}}(s)$ and with all rotational symmetry numbers set to unity. All the kinetics calculations were carried out using the POLYRATE 7.8 program.[22] The rotational partition functions were calculated classically, while the vibrational modes were treated quantum mechanically as separable harmonic oscillators. Spin−orbit splitting of O (^{3}P), $^3P_0$, $^3P_1$, and $^3P_2$ was considered in calculating electron partition functions. A correction method considering the centrifugal-dominant small-curvature tunneling effect[20] was used in the rate constant calculation. Methods for large curvature cases[23] were not used in this work, as they require more information about the PES, beyond the scope of this work.

3. Results and Discussion

The optimized geometries of the reactant, saddle points, and products are shown in Figure 1 for the reaction of O (^{3}P) with CH_3CHF_2. The vibrational frequencies of the reactant, products, and saddle points are listed in Table 1. The calculated classical potential barriers ΔE and the reaction enthalpies ΔH are summarized in Table 2. Figure 2 (a−b) shows the classical potential energy (V_{MEP}) and vibrationally adiabatic potential energy (V_a^{G}) curves as functions of distance along the reaction coordinate s at the QCISD(T)/6-311+G(3df,2p)//MP2/6-311G(d,p) level. The calculated TST, CVT, and CVT/SCT rate constants along with the experimental values are presented in Table 3 and Figure 3 over the temperature range of 200∼3000 K.

3.1 Reaction Mechanism. The reactions of O (^{3}P) with haloalkanes are the prototype of simple metathesis reactions in which a hydrogen atom is transferred via an apparent barrier in the reaction coordinate. For the reaction of O (^{3}P) with CH_3CHF_2, two primary processes have been identified:

$$CH_3CHF_2 + O \rightarrow CH_2CHF_2 + OH$$

H abstraction from the CH_3 group

$$CH_3CHF_2 + O \rightarrow CH_3CF_2 + OH$$

H abstraction from the CH group

(a) H Abstraction from the CH_3 Group. At first, we located a saddle point under the assumption of C_1 symmetry, but resulting in a structure with C_s symmetry. It means that the O (^{3}P) atom approaches one of H atoms in the CH_3 group in C_s symmetry. This reaction can therefore proceed on two potential energy surfaces,^{3}A″ and ^{3}A′, because of the splitting of a degenerate O (^{3}P) state in the C_s symmetry. Both PESs adiabatically correlate with the products states ^{3}A″ and ^{3}A′. Indeed, for C_s symmetry the irreducible representation is ^{3}A′+ ^{3}A″(2) for reactants and ^{3}A′ + ^{3}A″ + ^{1}A′ + ^{1}A″ for products, and therefore, both asymptotes adiabatically correlate through the PESs ^{3}A′ and ^{3}A″ in C_s.

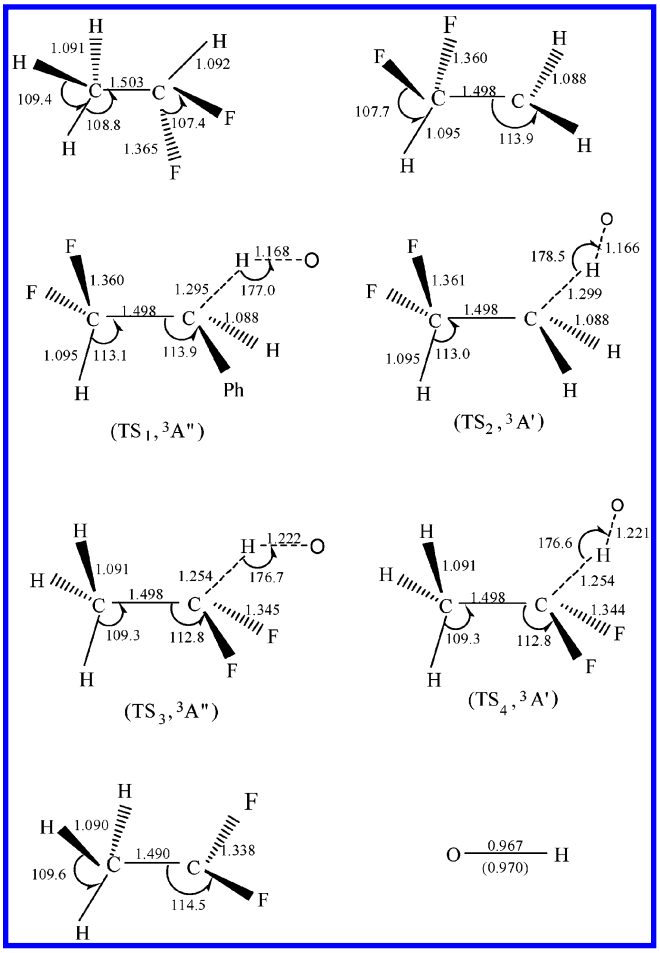

Figure 1. Geometries optimized at MP2/6-311G(d,p) level of theory for the stationary points. Distances are in angstroms, and angles are in degrees.

At the MP2/6-311G(d,p) level, two saddle points with ^{3}A″ and ^{3}A′ symmetries were located for the channel of H abstraction from the CH_3 group, whose geometrical structures are shown in Figure 1. The saddle points of ^{3}A″ and ^{3}A′symmetries are denoted as TS_1 and TS_2, respectively. At the QCISD(T)/6-311+G(3df,2p)//MP2/6-311G(d,p) level, the barrier heights are 12.63 and 12.74 kcal/mol on the ^{3}A″ and ^{3}A′ potential surfaces, reactively. Therefore, the energy difference between TS_1 and TS_2 is only 0.32 kcal/mol. Population analysis shows that the half-filled p-orbital of the ^{3}A″ symmetry is in CCHO plane and the half-filled p-orbital of the ^{3}A′ symmetry is perpendicular to this plane. The O (^{3}P) atom abstracts one of the H atoms from the CH_3 group either from the *trans*-position of the other C atom via TS_1 on the ^{3}A″ surface or from *cis*-position via TS_2 on the ^{3}A′ surface. The breaking C−H bonds are elongated by 18.70% and 19.07%, while the forming O−H bonds are longer than the equilibrium value of 0.967 Å in OH radical by 20.79% and 20.58% for the saddle points of ^{3}A″ and ^{3}A′ symmetries. This result indicates that the barrier of the

TABLE 1: The Calculated Vibrational Frequencies (in cm^{-1}) for the Reactant, Products, and Saddle Points Involved in the Reaction of O (^3P) with CH_3CHF_2 at the MP2/6-311G(d,p) Level[a]

species	frequencies										
CH_3CHF_2	3207	3205	3150	3103	1509	1507	1471	1441	1410	1189	1185
	1178	978	893	577	475	389	258				
	3016	*3001*	*2975*	*2959*	*1457*	*1451*	*1413*	*1364*	*1360*	*1171*	*1145*
	1135	*942*	*869*	*570*	*471*	*391*	*221*				
CH_2CHF_2	3362	3233	3107	1486	1436	1409	1188	1181	1008	936	654
	502	427	400	140							
CH_3CF_2	3220	3180	3078	1498	1498	1438	1303	1278	1119	998	886
	554	474	380	209							
TS_1	3261	3164	3121	1478	1439	1419	1250	1240	1179	1173	1045
	971	883	593	569	488	484	375	85	75[b]	2241i	
TS_2	3266	3165	3122	1479	1439	1419	1287	1211	1176	1138	1090
	961	904	621	581	488	415	367	99	69[b]	2256i	
TS_3	3209	3207	3103	1500	1492	1437	1339	1301	1217	1189	1147
	995	894	660	498	405	385	242	101	61[b]	2421i	
TS_4	3211	3205	3102	1502	1501	1438	1351	1280	1218	1177	1169
	1000	897	659	501	406	387	242	145	117[b]	2419i	
OH	3852										
	3735										

[a] The values in italics are the experimental data.[24] [b] The lowest-frequency vibrations of the saddle points are considered as internal rotations.[25]

hydrogen abstraction from the CH_3 group is almost centrally located, as expected for a weakly endothermic reaction.

Each saddle point is identified with one negative eigenvalue of the respective Hessian matrix and therefore, one imaginary frequency. Since the imaginary frequency governs the width of the classical potential energy barrier along the MEP, it plays an important role in the tunneling calculations, especially when the imaginary frequency is large, and the associated eigenvector has a large component of hydrogenic motion. For the channel of H abstraction from the CH_3 group, the imaginary frequencies of TS_1 and TS_2 are 2241i and 2256i, so we expect that the tunneling effect should be important for the calculation of the rate constant. Direct inspection of the saddle point low-frequency mode indicates that, in both cases, the mode of the lowest frequency (75 and 69 cm^{-1}) is a hindered internal rotation instead of a small-amplitude vibration. The mode was removed from the vibrational partition function for the saddle point and the corresponding hindered rotor partition function $Q_{HR}(T)$, calculated by the method devised by Truhlar,[25] was included in the expression of the rate constant.

(b) H Abstraction from the CH Group. The channel of H abstraction from the CH group also proceeds on two potential energy surfaces with $^3A''$ and $^3A'$ symmetries, which is similar to the channel of the hydrogen abstraction from the CH_3 group. At the MP2/6-311G(d,p) level, two distinct saddle points TS_3 ($^3A''$, with half-filled p-orbital in the CCHO plane) and TS_4 ($^3A'$, with half-filled p-orbital perpendicular to the CCHO plane) were found for the channel of H abstraction from the CH group. The corresponding barrier heights are calculated to be 12.63 and 12.74 kcal/mol, respectively. Therefore, the energy difference between TS_3 and TS_4 is only 0.11 kcal/mol. It implies that the states are nearly degenerate. The breaking C−H bonds are elongated by 14.94% and 14.94%, while the forming O−H bonds are longer than the equilibrium value of 0.967 Å by 26.37% and 26.27% for the saddle points of $^3A''$ and $^3A'$ symmetries. Therefore, these two saddle points are reactant-like, and hydrogen abstraction from the CH group via early potential barrier. As shown in Table 1, the saddle points of $^3A''$ and $^3A'$ symmetries have very similar vibrational frequencies, in accordance with their very similar geometrical parameters and total energies. The similarity of the two saddle points in the geometries, frequencies, and energies allows us to assume that the kinetic nature for both $^3A''$ and $^3A'$ surfaces will be very similar.

TABLE 2: The Calculated Classical Potential Barriers ΔE (in kcal/mol) and the Reaction Enthalpies ΔH (in kcal/mol) at the QCISD(T)/6-311+G(3df,2p)//MP2/6-311G(d,p) Level for All the Channels Involved in the Reaction of O (^3P) with CH_3CHF_2

energy	CH-attack	CH_3-attack
ΔE ($^3A'$)	12.74	17.42
ΔE ($^3A''$)	12.63	17.10
ΔH	−2.18	7.30

At the QCISD(T)/6-311+G(3df,2p)//MP2/6-311G(d,p) level, the potential barrier of H abstraction from the CH_3 group is about 5 kcal/mol higher than that of the hydrogen abstraction from the CH group. Thus, the hydrogen abstraction from the CH group is the dominant channel for the reaction of O (^3P) with CH_3CHF_2. Whereas the hydrogen abstraction from the CH group is an exothermic reaction ($\Delta H = -2.18$ kcal/mol), the H abstraction from the CH_3 group is an endothermic reaction ($\Delta H = 7.30$ kcal/mol).

3.2 The Kinetics Calculation. For each channel, the rate constants of the $^3A''$ and $^3A'$ surfaces have been calculated independently. The two surfaces show similar features and further discussion in this paper will refer only to $^3A''$ surface.

The minimum energy path (MEP) was calculated at the MP2/6-311G(d,p) level by the IRC definition. In our kinetics calculation, the MEP is taken as the reaction path. For both channels, the maximum position of the classical potential energy V_{MEP} curve at the QCISD(T)/6-311+G(3df,2p)//MP2/6-311G(d,p) level corresponds to the saddle point structure at the MP2/6-311G(d,p) level. Therefore, the shifting of the maximum position for the V_{MEP} curve caused by the computational technique (artificial variational effect) is avoided. The changes of the classical potential energy V_{MEP} and the ground-state vibrational adiabatic potential energy V_a^G with the reaction coordinate s on the $^3A''$ potential surface are shown in Figure 2 (a−b) for the two channels of H abstraction from the CH_3 and CH groups. For each channel, the V_{MEP} and V_a^G curves are similar in shape, and their maximum positions are almost the same at the QCISD(T)/6-311+G(3df,2p)//MP2/ 6-311G(d,p) level. The zero-point energy ZPE, which is the difference of V_a^G and V_{MEP}, shows little change with the reaction coordinate s, indicating that the variational effect will be small for this reaction.

The canonical variational transition-state theory (CVT) with a small-curvature tunneling correction (SCT) has been success-

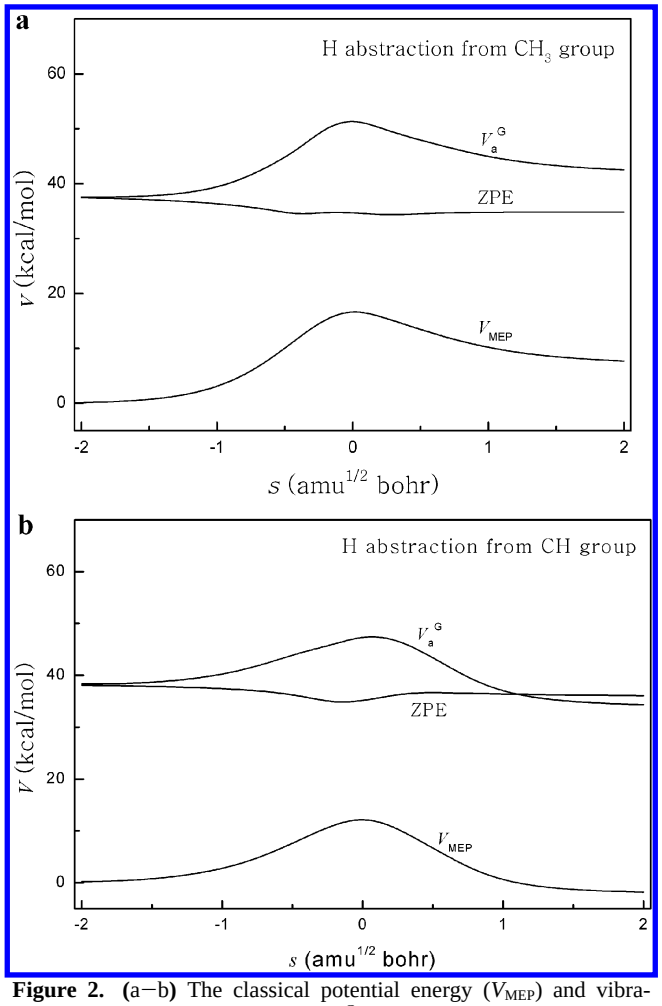

Figure 2. **(**a−b**)** The classical potential energy (V_{MEP}) and vibrational adiabatic potential energy (V_a^G) curves as functions of s at the QCISD(T)/6-311+G(3df,2p)// MP2/6-311G(d,p) level on the ^{3}A″ potential energy surface.

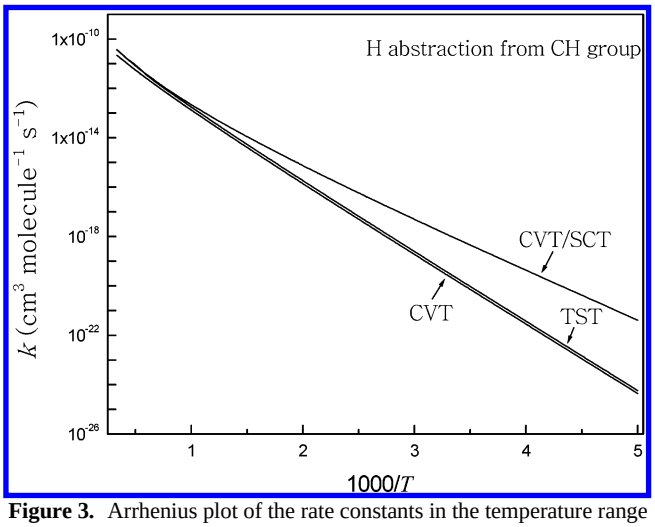

Figure 3. Arrhenius plot of the rate constants in the temperature range of 200∼3000 K for the channel of H abstraction from the CH group.

fully performed for several analogous reactions.[26−27] It is an efficient method to calculate the rate constant. In this paper, we used this method to calculate the rate constants for the reaction of O (^{3}P) with CH_3CHF_2 over a wide temperature range from 200 to 3000 K.

To calculate the rate constant, 30 points were selected near the saddle point along the MEP, 15 points in the reactant zone and 15 points in the product zone. The CVT/SCT rate constants

TABLE 3: The Calculated CVT/SCT Rate Constants and the Branching Ratios along with the Experimental Values[13] for All the Channels Involved in the Reaction of O (^{3}P) with CH_3CHF_2

T/K	k_1	k_2	k	k_1/k	k_2/k	exptl
200	1.81E-26	4.10E-22	4.10E-22	0.00	1.00	
250	1.51E-23	4.26E-20	4.26E-20	0.00	1.00	
298	1.21E-21	8.96E-19	8.97E-19	0.00	1.00	
300	1.42E-21	9.96E-19	9.97E-19	0.00	1.00	
350	3.78E-20	9.93E-18	9.97E-18	0.00	1.00	
400	4.61E-19	5.79E-17	5.84E-17	0.01	0.99	
450	3.33E-18	2.36E-16	2.39E-16	0.01	0.99	
500	1.66E-17	7.42E-16	7.59E-16	0.02	0.98	
600	1.97E-16	4.39E-15	4.58E-15	0.04	0.96	
700	1.22E-15	1.65E-14	1.78E-14	0.07	0.93	
800	5.02E-15	4.67E-14	5.17E-14	0.10	0.90	
900	1.56E-14	1.08E-13	1.24E-13	0.13	0.87	
1000	3.98E-14	2.18E-13	2.57E-13	0.15	0.85	
1100	4.11E-13	9.02E-14	5.01E-13	0.18	0.82	9.53E-13
1150	5.06E-13	1.19E-13	6.25E-13	0.19	0.81	1.30E-12
1200	1.71E-13	6.57E-13	8.28E-13	0.21	0.79	1.87E-12
1250	8.12E-13	2.21E-13	1.03E-12	0.21	0.79	2.60E-12
1300	1.01E-12	2.92E-13	1.30E-12	0.22	0.78	3.53E-12
1340	1.18E-12	3.60E-13	1.54E-12	0.23	0.77	4.44E-12
1400	5.13E-13	1.52E-12	2.03E-12	0.25	0.75	
1600	1.21E-12	3.07E-12	4.28E-12	0.28	0.72	
1800	2.44E-12	5.12E-12	7.56E-12	0.32	0.68	
2000	4.35E-12	8.35E-12	1.27E-11	0.34	0.66	
2200	7.11E-12	1.21E-11	1.92E-11	0.37	0.63	
2400	1.09E-11	1.69E-11	2.78E-11	0.39	0.61	
2600	1.57E-11	2.28E-11	3.85E-11	0.41	0.59	
2800	2.18E-11	2.95E-11	5.13E-11	0.42	0.58	
3000	2.91E-11	3.76E-11	6.67E-11	0.44	0.56	

and the branching ratios of each channel are listed in Table 3. For the purpose of comparison, the experimental rate constants are also show in Table 3. The rate constants of each channel are obtained as the sum of the calculated CVT/SCT rate constants of the ^{3}A″ and ^{3}A′ surfaces. The CVT/SCT rate constants of the channel of H abstraction from the CH group are noted as k_1, while the rate constants of H abstraction from the CH_3 group are noted as k_2. The total rate constants of the reaction of O (^{3}P) with CH_3CHF_2 are noted as k, with $k = k_1 + k_2$. The branching ratios of the channels of H abstraction from the CH and CH_3 groups are noted as k_1/k and k_2/k, respectively.

Because of the presence of the smaller potential barrier, H abstraction from the CH group is the dominant reaction channel over the whole temperature range. In the temperature range of 200∼500 K, the rate constants for attack at the CH_3 group are so small that it can be negligible. Thus, the channel of H abstraction from the CH group is the sole channel. However, as the temperature increases, H abstraction from the CH_3 group becomes a competitive reaction channel. When $T > 500$ K, the rate constant k_2 cannot be considered to be negligible and will account for some branching ratio to the overall rate constants. For example, at $T = 2000$ K, $k_2/k = 0.34$.

Over the temperature range of 1100∼1340 K, the total CVT/SCT rate constants, which is the sum of the CVT/SCT rate constants for all the channels, are in good agreement with the experimental values.[13] Therefore, the CVT/SCT rate constants are taken as the accurate rate constants for each channel.

At low temperature, the rate constants for the reaction of O (^{3}P) with CH_3CHF_2 are relatively small. Therefore, this reaction cannot occur to any significant extent under the atmospheric condition. However, the rate constants increase rapidly with elevation of temperature. At 3000 K, the CVT/SCT rate constant of this reaction is 6.67×10^{-11} cm^3 molecule^{-1} s^{-1}. So the reaction should play an important role under high-temperature combustion conditions.

To compare further the CVT/SCT rate constants with the TST and CVT rate constants of the conventional transition state theory, Figure 3 shows the calculated TST, CVT, and CVT/SCT rate constants against the reciprocal of the temperature for the channel of H abstraction from the CH group. Several important features of the calculated rate constants are summarized as follows.

(1) The values of TST rate constants and those of CVT rate constants are nearly the same, which enables us to conclude that the variational effect is small for the calculation of the rate constants. This conclusion is in good agreement with the above analysis. The same conclusion can be drawn from the channel of the hydrogen abstraction from the CH_3 group.

(2) Reactions involving hydrogen atom transfer are usually characterized with significant tunneling effect that must be accounted for when computing reaction rate constants. In the present case, the CVT/SCT rate constants are greater than the CVT ones over the temperature range of 200∼800 K; for example, at 298 K, the CVT rate constant is 1.84×10^{-20} cm^3 molecule^{-1} s^{-1}, while the CVT/SCT rate constant is 8.96×10^{-19} cm^3 molecule^{-1} s^{-1}. The latter is 48.70 times larger than the former. However, the difference between the CVT rate constant and the CVT/SCT rate constant decreases with the increase in temperature. When the temperature is higher than 800 K, the CVT/SCT rate constants are asymptotic to the rate constants of CVT, which means only in the lower temperature range the small curvature tunneling correction plays an important role for the calculation of the rate constant. The same conclusion can be drawn from the hydrogen abstraction from the CH_3 group.

(3) The calculated rate constants exhibit typical non-Arrhenius behavior. The CVT/SCT rate constants of each channel and the total rate constants are fitted by three-parameter formulas over the temperature range of 200∼3000 K and are given in units of cm^3 molecule^{-1} s^{-1} as follows:

$$k_1(T) = (2.94 \times 10^{-18})T^{2.22} \exp(-4127.75/T)$$

for H abstraction from the CH group

$$k_2(T) = (2.69 \times 10^{-18})T^{2.28} \exp(-6180.40/T)$$

for H abstraction from the CH_3 group

$$k(T) = (1.46 \times 10^{-19})T^{2.66} \exp(-3986.80/T)$$

for the total rate constants

4. Conclusion

The comprehensive study on the reaction of O (^{3}P) with CH_3CHF_2 using ab initio and canonical variational transition-state theory (CVT) with small-curvature tunneling effect has led to the following specific conclusions.

(1) This reaction involves two channels: H abstraction from the methyl group (CH_3) and H abstraction from the methyne group (CH). At the lower temperatures, the hydrogen abstraction from the CH group is the sole channel. With increasing temperature, the hydrogen abstraction from the CH_3 group becomes a competitive channel.

(2) The variational effect is small for all the channels.

(3) The small curvature tunneling contribution plays an important role for the calculation of the rate constants over the low-temperature range.

(4) Rate constants were reported over the temperature range of 200∼3000 K. The CVT/SCT overall rate constant is in good agreement with the experimental values over the temperature range of 1100∼1340 K.

Acknowledgment. The authors thank Professor Donald G. Truhlar for providing the POLYRATE 7.8 program.

References and Notes

(1) Tuck, R.; Plumb, A.; Condon, E. *Geophys. Res. Lett.* **1990**, *17*, 313.
(2) Manzer, L. *Science* **1990**, *249*, 31.
(3) Atkinson, R. *Chem. Rev.* **1986**, *86*, 69.
(4) Warnatz, J. I. *Combustion Chemistry*; Gardiner, W. C., Jr., Ed. Spinger-Verlag: New York, 1984.
(5) Smith, K. M.; Duxburg, G.; Newnham, D. A.; Ballard, J. *J. Chem. Soc., Faraday Trans.* **1997**, *93*, 2735.
(6) Miziolek, A. W.; Tsang, W. *Halon Replacements: Technology and Science*; ACS Symposium Series 611; American Chemical Society: Washington, DC, 1995.
(7) Kneba, M.; Wolfrum, J. *Bunsen-Ges., Ber. Phys. Chem.* **1977**, *81*, 1275.
(8) Su, M.-C.; Lim, K. P.; Michael, J. V. *J. Phys. Chem.* **1994**, *98*, 8411.
(9) Westenberg, A. A.; DeHaas, N. *J. Chem. Phys.* **1975**, *62*, 4477.
(10) Jourdain, J. L.; Poulet, G.; Barassin, J.; LeBras, G.; Combourieu, J. *Pollution Atmospheric* **1977**, *75*, 256.
(11) Herron, J. T. *J. Phys. Chem. Ref. Data* **1988**, *17*, 967.
(12) Barassin, J.; Richoux, M.; Combourieu, J. *Bull. Soc. Chim. Fr.* **1977**, 69.
(13) Shiina, H.; Tsuchiya, K.; Oya, M.; Miyoshi, A.; Matsui, H. *Chem. Phys. Lett.* **2001**, *36*, 242.
(14) Zhang, Q. Z.; Wang, S. K.; Gu, Y. S. *New J. Chem.* **2003**, *27*, 289
(15) Lu, W. C.; Zhang, R. Q.; Wong, N. B. *J. Phys. Chem. B* **2003**, *107*, 2061.
(16) Zhang, R. Q.; Lu, W. C.; Lee, S. T. *Appl. Phys. Lett.* **2002**, *88*, 4223.
(17) Baldridge, K. K.; Gordor, M. S.; Steckler, R.; Truhlar, D. G. *J. Phys. Chem.* **1989**, *93*, 5107.
(18) Gonzalez-Lafont, A.; Truong, T. N.; Truhlar, D. G. *J. Chem. Phys.* **1991**, *95*, 8875.
(19) Garrett, B. C.; Truhlar, D. G. *J. Phys. Chem.* **1979**, *83*, 1052.
(20) Liu, Y.-P.; Lynch, G. C.; Truong, T. N.; Lu, D.-H.; Truhlar, D. G.; Garrett, B. C. *J. Am. Chem. Soc.* **1993**, *115*, 2408.
(21) Frisch, M. J.; Trucks, G. W.; Schlegel, H. B.; Scuseria, G. E.; Robb, M. A.; Cheeseman, J. R.; Zakrzewski, V. G.; Montgomery, J. A., Jr.; Stratmann, R. E.; Burant, J. C.; Dapprich, S.; Millam, J. M.; Daniels, A. D.; Kudin, K. N.; Strain, M. C.; Farkas, O.; Tomasi, J.; Barone, V.; Cossi, M.; Cammi, R.; Mennucci, B.; Pomelli, C.; Adamo, C.; Clifford, S.; Ochterski, J.; Petersson, G. A.; Ayala, P. Y.; Cui, Q.; Morokuma, K.; Malick, D. K.; Rabuck, A. D.; Raghavachari, K.; Foresman, J. B.; Cioslowski, J.; Ortiz, J. V.; Baboul, A. G.; Stefanov, B. B.; Liu, G.; Liashenko, A.; Piskorz, P.; Komaromi, I.; Gomperts, R.; Martin, R. L.; Fox, D. J.; Keith, T.; Al-Laham, M. A.; Peng, C. Y.; Nanayakkara, A.; Gonzalez, C.; Challacombe, M.; Gill, P. M. W.; Johnson, B.; Chen, W.; Wong, M. W.; Andres, J. L.; Gonzalez, C.; Head-Gordon, M.; Replogle, E. S.; Pople, J. A. *Gaussian 98*, Revision A.7; Gaussian, Inc.: Pittsburgh, PA, 1998.
(22) Steckler, R.; Chuang, Y. Y.; Fast, P. L.; Corchade, J. C.; Coitino, E. L.; Hu, W. P.; Lynch, G. C.; Nguyen, K.; Jackells, C. F.; Gu, M. Z.; Rossi, I.; Clayton, S.; Melissas, V.; Garrett, B. C.; Isaacson, A. D.; Truhlar, D. G. *POLYRATE*, Version 7.8; University of Minnesota: Minneapolis, MN, 1997.
(23) Truong, T. N.; Lu, D.-H.; Lynch, G. C.; Liu, Y. P.; Melissas, V. S.; Stewart, J. J.; Steckler, R.; Garrett, B. C.; Isaacson, A. D.; Gonzalez-Lafont, A.; Rai, S. N.; Hancock, G. C.; Joseph, T.; Truhlar, D. G. *Comput. Phys. Commun.* **1993**, *75*, 43.
(24) McNaughton, D.; Evans, C. *J. Phys. Chem.* **1996**, *100*, 8660.
(25) Truhlar, D. G. *J. Comput. Chem.* **1991**, *12*, 266.
(26) Melissas, V. S.; Truhlar, D. G. *J. Chem. Phys.* **1993**, *99*, 1013.
(27) Corchado, J. C.; Espinosa-Garcia, J.; Roberto-Neto, O.; Chuang, Y.-Y.; Truhlar, D. G. *J. Phys. Chem. A* **1998**, *102*, 4899.